Bioinformatics analysis indicates that microRNA-628-5p overexpression may alleviate Alzheimer's disease by targeting TYROBP

MIAO LIU[1,2], SHULING LI[2,3], CHUN MA[2,3], XINNA WANG[1,2], YU SHUANG[1,2], HAINING LIN[1,2], ZHIYING GUAN[1,2] and LIHUA YANG[2,3]

[1]College of Traditional Chinese Medicine, Changchun University of Chinese Medicine; [2]Research Center of Changchun University of Chinese Medicine; [3]Department of Geriatrics, Affiliated Hospital of Changchun University of Chinese Medicine, Changchun, Jilin 130021, P.R. China

Received March 31, 2020; Accepted October 30, 2020

DOI: 10.3892/mmr.2020.11781

Abstract. Alzheimer's disease (AD) is a global health issue, but the precise underlying mechanism has not yet been elucidated. The present study aimed to integrate microRNA (miRNA or miR) and mRNA profiles of AD and identify hub genes via bioinformatics analysis. Datasets associated with AD (GSE113141, GSE104249 and GSE138382) were integrated. Bioinformatics analysis was used to identify the hub mRNAs. TargetScan was used to predict miRNAs that have binding sites for the hub genes. Reverse transcription-quantitative (RT-q)PCR and western blot analysis was performed to assess miRNA and mRNA expression levels in APP/PS1 transgenic mice and human U251 cells. Luciferase reporter assay and RNA interference were utilized to verify the functions of these miRNAs *in vitro*. Bioinformatics analysis demonstrated that expression levels of the gene encoding transmembrane immune signaling adaptor *TYROBP* were upregulated in both the GSE113141 and GSE104249 datasets; *TYROBP* also served as the hub gene in AD. miR-628-5p was predicted to have binding sites for *TYROBP* and was downregulated in GSE138382. RT-qPCR confirmed low miR-628-5p and high TYROBP expression levels in APP/PS1 transgenic mice and human U251 cells. Western blot analysis demonstrated high protein expression levels of amyloid β (Aβ) precursor protein, Aβ and TYROBP in APP/PS1 transgenic mice and U251 cells. Dual luciferase reporter assay confirmed that TYROBP was targeted by miR-628-5p. miR-628-5p/TYROBP may inhibit progressive neurodegeneration in AD and could be used as novel biomarkers and candidate drug targets.

Correspondence to: Dr Lihua Yang, Department of Geriatrics, Affiliated Hospital of Changchun University of Chinese Medicine, 1478 Gongnong Road, Changchun, Jilin 130021, P.R. China
E-mail: ylh7239@126.com

Abbreviations: BP, biological processes; CC, cellular component; DEGs, differentially expressed genes; GO, Gene Ontology; KEGG, Kyoto Encyclopedia of Genes and Genomes; MF, molecular function; PPI, protein-protein interaction; RT-q, reverse transcription-quantitative

Key words: Alzheimer's disease, mRNA, microRNA

Introduction

Alzheimer's disease (AD) has become a global health issue; >44 million people are currently living with AD and the global health care cost in 2010 was ~US$818 billion (1). AD is a severe neurodegenerative disease associated with progressive cognitive decline (2). The pathogenesis of AD is complex, and the precise underlying mechanism has not yet been elucidated. The amyloid hypothesis is widely accepted for the pathogenesis of AD (3). As per this hypothesis, accumulation of β-amyloid (Aβ) peptides in brain cells is the primary pathological change in AD. Therefore, drugs such as Semagacestat (4) and Tramiprosate (5) targeting inhibition of Aβ aggregation have been developed. However, no significant therapeutic effects have been observed in phase III trials of these drugs (6). Thus, identifying the precise molecular mechanisms of AD progression is necessary.

Transmembrane immune signaling adaptor TYROBP (TYROBP) is a type I transmembrane protein expressed in numerous types of immune cell, such as osteoclasts, macrophages and monocytes (7). The gene encoding TYROBP is located on the long arm of chromosome 19 at position 13.1 and contains five exons (8). TYROBP is a necessary component of activating signal transduction (9). It is typically expressed on microglial cells in the brain (10). Certain TYROBP-associated immune receptors, such as triggering receptor expressed on myeloid cells (TREM)2, signal regulatory protein β1 and complement receptor (CR)3, have been identified (10). The interaction between spleen tyrosine kinase and phosphorylated TYROBP leads to intracellular calcium mobilization and modulates immune cell function (11). In addition, TYROBP suppresses the inflammatory response by downregulating cytokine production and secretion (12). TYROBP-mediated signaling is considered to participate in regulating the

expression levels of multiple genes, including TREM1 and TREM2, in the brain (13).

Modern second-generation sequencing technology can reveal genetic changes between healthy individuals and patients (14). This technique has been used in AD to identify a number of relevant genes such as TREM1 and TYROBP (15). However, owing to the large number of altered genes, a single AD-promoting gene in AD has not been identified. Bioinformatics analysis for identifying hub genes may facilitate the identification of key diagnosis biomarkers and molecular drug targets (16). Before bioinformatics analysis, exclusion of irrelevant information caused by individual differences (17) is necessary. In addition, bioinformatics analysis results need to be verified experimentally.

The present study integrated two AD profiles and analyzed the co-expression of differentially expressed genes (DEGs) in both profiles. Bioinformatics analysis was used to identify the hub genes and relevant microRNAs (miRNAs or miRs). Finally, the function of these identified miRNAs in AD was verified experimentally.

Materials and methods

Preliminary analysis of GSE113141 (18) and GSE104249 (19). A total of two AD profiles were acquired from the Gene Expression Omnibus database (ncbi.nlm.nih.gov/gds/): GSE113141, containing information from six APP/PS1 transgenic and six normal mice, and GSE104249, containing information from three APP/PS1 transgenic and three normal mice. R software (version R 3.2.3) (20) and R studio (version R 3.5.2) (21) with the LIMMA package was used for homogenizing the raw data and identifying co-expressed DEGs.

Bioinformatics analysis. The Database for Annotation, Visualization and Integrated Discovery online tool (david.ncifcrf.gov/summary.jsp) was used for Gene Ontology (GO; https://david.ncifcrf.gov/) and Kyoto Encyclopedia of Genes and Genomes (KEGG; https://david.ncifcrf.gov/) (22) pathway analysis of all co-expressed DEGs. These genes were used as input for the Search Tool for the Retrieval of Interacting Genes/Proteins (STRING) database (string-db.org/cgi/input.pl) to acquire a protein-protein interaction (PPI) network, and Cytoscape (23) was used to visualize the network. The cytoHubba plugin in Cytoscape (version 3.6.1) was used to calculate the hub genes of AD. GeneMANIA (genemania.org/) was used to identify the interactions between the co-expressed genes. TargetScan (targetscan.org/) was utilized to predict the relevant miRNAs that bind the hub gene. All the predicted miRNAs were integrated with GSE138382, a miRNA gene profile associated with AD containing information from three APP/PS1 transgenic mice and three normal mice.

Reverse transcription-quantitative (RT-q)PCR validation. RNA (from cells, tissues and blood) was extracted using TRIzol® reagent (Invitrogen; Thermo Fisher Scientific, Inc.). NanoDrop ND-1000 (Thermo Fisher Scientific, Inc.) was used to detect the integrity and concentration of the RNA samples. Total RNA was reverse-transcribed to cDNA using PrimeScript RT reagent kit with gDNA Eraser (Takara Bio, Inc.) according to the manufacturer's instructions. RT-qPCR was performed using FastStart Universal SYBR Green Master (ROX) (Roche Diagnostics) using an Applied Biosystems 7500 Fast Real-Time PCR system (Applied Biosystems; Thermo Fisher Scientific, Inc.) to confirm the relative expression levels of miR-628-5p and *TYROBP* in mouse brain tissue. In addition, *TYROBP* and miR-628-5p were detected in blood samples from patients with AD. qPCR thermocycling conditions were 95˚C for 5 min, followed by 40 cycles at 95˚C for 10 sec, 55˚C for 20 sec and 72˚C for 20 sec with an extension step of 72˚C for 2 min. Results were normalized to those of U6 or GAPDH and calculated using the $2^{-\Delta\Delta Cq}$ (24) method. The primers were as follows: Human TYROBP forward, 5'-ACTGAGACCGAG TCGCCTTAT-3' and reverse, 5'-ATACGGCCTCTGTGTGTT GAG-3'; moue TYROBP forward, 5'-GAGTGACACTTTCCC AAGATGC-3' and reverse, 5'-CCTTGACCTCGGGAGACC A-3'; human GAPDH forward, 5'-CGGACCAATACGACC AAATCCG-3' and reverse, 5'-AGCCACATCGCTCAGACA CC-3'; mouse GAPDH forward, 5'-AGGTCGGTGTGAACG GATTTG-3' and reverse, 5'-GGGGTCGTTGATGGCAAC A-3'; human miR-628-5p forward, 5'-GATGCTGGATGC TGACATATTTAC-3' and reverse, 5'-TATGGTTGTTCTGCT CTCTGTCTC-3'; and U6 forward, 5'-GCGCGTCGTGAA GCGTTC-3' and reverse, 5'-GTGCAGGGTCCGAGGT-3'.

Participants. The present study was performed in accordance with the Declaration of Helsinki and was approved by the Ethics Committee of Changchun University of Chinese Medicine (Changchun, China; approval no. IRB:2019024421). Blood (4 ml) was obtained from median cubital vein of patients with AD or healthy controls in Department of Geriatrics or Medical Examination Center (Affiliated Hospital to Changchun University of Chinese Medicine, Changchun, China). The participants were enrolled between February 2019 and July 2019. The inclusion and exclusion criteria of AD was based on the criteria from the National Institute of Neurological and Communicative Diseases and Stroke-Alzheimer's Disease and Related Disorders Association (25). Participants were divided into two groups, AD and healthy control, based on the criteria from the National Institute of Neurological and Communicative Diseases and Stroke-Alzheimer's Disease and Related Disorders Association (25). Blood samples were collected from 20 participants, including 10 patients with AD and 10 healthy controls. The AD group comprised six females and four males (age, 71-87 years; mean age, 77.6±4.6 years). The control group comprised five females and five males (age, 73-82 years; mean age, 76.9±2.7 years). All patients agreed to the use of their samples in scientific research and provided written informed consent.

Animals. Male 6-month-old APP/PS1 (n=3) and C57/6J (normal) (n=3) mice (weight 24-28 g) were purchased from the Chinese Academy of Medical Sciences (Shanghai, China). All mice were housed in 12 h light/dark cycle conditions at a temperature of 22±1˚C and a humidity of 55±2% and given food and water *ad libitum*. All mice were anesthetized with isoflurane (induction, 5%; maintenance, 1.5-2.5%). The hippocampus and cortex were dissected for subsequent experiments, including RT-qPCR and western blotting. Then all the mice were euthanized via cervical dislocation. Animal experiments were performed in accordance with the National Institutes of

Health Guide for the Care and Use of Laboratory Animals (26) and approved by The Changchun University of Chinese Medicine Animal Care and Use Committee (Changchun, China; approval no. KT202009096).

Cell culture. U251 glioblastoma cells were purchased from Institute of Biochemistry and Cell Biology and cultured in DMEM (Gibco; Thermo Fisher Scientific, Inc.) with 10% FBS (cat. no. 0010; Gibco; Thermo Fisher Scientific, Inc.) at 37˚C in a humidified 5% CO_2 incubator. The medium was replaced every 3 days. Mimic and inhibitor were designed by Shanghai GenePharma Co., Ltd. For transfection of miR-628-5p mimics (250 pmol; forward, 5'-AUGCUGACAUAUUUACUAGAG G-3' and reverse, 5'-UCUAGUAAAUAUGUCAGCAUUU-3') and inhibitor (250 pmol, 5'-CCUCUAGUAAAUAUGUCA GCAU-3'), cells were transfected with Lipofectamine® 2000 (Invitrogen; Thermo Fisher Scientific, Inc.). In the control group, cells were transfected with Lipofectamine® 2000 alone. The time interval between transfection and subsequent experimentation was 48 h. After media was replaced with serum-free Opti-MEM (Gibco; Thermo Fisher Scientific, Inc.), the transfection complexes were added for 6 h at 37˚C in a humidified 5% CO_2 incubator. Then the medium was replaced with the standard culture medium (DMEM with 10% FBS) and cells harvested following incubation for 48 h at 37˚C.

Western blotting. The protein was extracted using RIPA buffer (Beijing Solarbio Science & Technology Co., Ltd.) and quantified using a BCA assay (Thermo Fisher Scientific, Inc.). Total cell protein content (30 μg/lane) was separated by 10% SDS-PAGE (cat. no. 1200; Beijing Solarbio Science & Technology Co., Ltd.) and transferred to nitrocellulose membranes (0.45 μm; EMD Millipore). Blots were blocked using 5% non-fat milk with 0.1% Tween-20 (Sigma-Aldrich; Merck KGaA) for 2 h at 37˚C. Diluted antibodies against TYROBP (cat. no. ab124834), Aβ (cat. no. ab224275)and Aβ precursor protein (APP; cat. no. ab32136; all at 1:1,000 and all from Abcam) were used to incubate the membranes overnight at 4˚C, followed by incubation with secondary antibody (β-actin; 1:5,000; cat. no. bs-0061R, Bioss) at room temperature for 2.5 h. The blots were then visualized with ECL using a Series Molecular Imaging Biosystem (Azure Biosystems, Inc.). Protein expression levels were semi-quantified using ImageJ software (version 4.62; National Institutes of Health).

Dual luciferase reporter assay. 293T cells were purchased from Institute of Biochemistry and Cell Biology. A total of $2x10^4$ 293T cells per well were seeded into 6-well plates for 24 h at 37˚C before transfection. The wild-type (WT) 3'-UTR sequence (16-23 bp) of TYROBP that can bind to miR-628-5p or the mutant (MUT) 3'-UTR sequence was amplified and then cloned into a pGL3 vector (Promega Corporation). pGL6-TYROBP-WT, pGL6-TYROBP-MUT and miR-628-5p mimics as well as mimic controls were co-transfected into 293T cells for 24 h at 37˚C using Lipofectamine® 2000 (Invitrogen; Thermo Fisher Scientific, Inc.). At 24 h post-transfection, the absorbance of the luciferase was measured at 560 nm. A dual luciferase reporter gene assay kit (Promega Corporation) was used to measure luciferase activities according to the manufacturer's protocol. Luciferase activity was normalized to *Renilla* luciferase.

Statistical analysis. Continuous data are expressed as the mean ± standard deviation. All experiments were performed in triplicate. One-way ANOVA followed by post hoc Tukey's test was performed to assess differences between multiple groups. All statistical analysis was performed using SPSS 22.0 software (IBM Corp.). $P<0.05$ was considered to indicate a statistically significant difference.

Results

Integration of GSE113141 and GSE104249. Raw data were normalized using R software and integrated (Fig. 1). The integration included information from nine APP/PS1 transgenic mice and nine normal mice. The genes co-expressed in both *GSE113141 and GSE104249* were selected. There were 22 different co-expressing mRNAs in both AD profiles, including Lyz1, Clec7a, Cybb, Thbs1, Pilra, Itgb2, Tyrobp, Rac2, Cst7, Lcp1, Klk6, Wfdc17, Top2a, Lilrb4a, Lyz2, Ctse, Ptprc, Cd36, Igsf6, Mpeg1, Tnni2 and Cd52. These 22 genes were subjected to bioinformatics analysis following homogenization. These results demonstrated that these 22 genes might participate in the progress of AD.

GO analysis. Co-expression of different mRNAs for biological processes ('immune system process' and 'defense response') was observed. The cellular component was associated with 'Extracellular space', 'Rough endoplasmic reticulum lumen' and 'Golgi *cis* cisterna'. The molecular function primarily corresponded to 'lysozyme activity', 'Low-density lipoprotein particle binding' and 'Transforming growth factor β binding' (Table I; Fig. 2). These results demonstrated that immune system process, rough endoplasmic reticulum lumen and lysozyme activity might participate in the progress of AD.

KEGG signaling pathway. All co-expressed DEG were enriched for 'phagosome' and 'malaria' (Fig. 3).

PPI network and hub genes. Interaction analysis using the STRING database demonstrated 22 nodes with 69 edges. These nodes and edges were utilized by Cytoscape for pictorial depiction of the network. The five hub genes predicted by CytoHubba analysis were those encoding TYROBP (score=14), cytochrome b-245 β chain (score=13), integrin sub-unit β 2 (score=12), protein tyrosine phosphatase receptor type C (score=12) and lysozyme 2 (score 11) (Fig. 4). GeneMANIA database also demonstrated that *TYROBP* served a central role in 'physical interactions', 'pathway', 'predicted' and 'co-expression' networks (Fig. 5A-D, respectively). These results demonstrated that the function of TYROBP acted as a hub gene in AD and required further investigation.

TargetScan prediction. TargetScan (version 7.2; www.targetscan.org/vert_72) was used to predict miRNAs that target *TYROBP* (Table SI). In total, there were 77 miRNAs having binding sites for *TYROBP*. Subsequent integration of GSE138382 with the 77 predicted miRNAs demonstrated only one miRNA, miR-628-5p, that was downregulated in

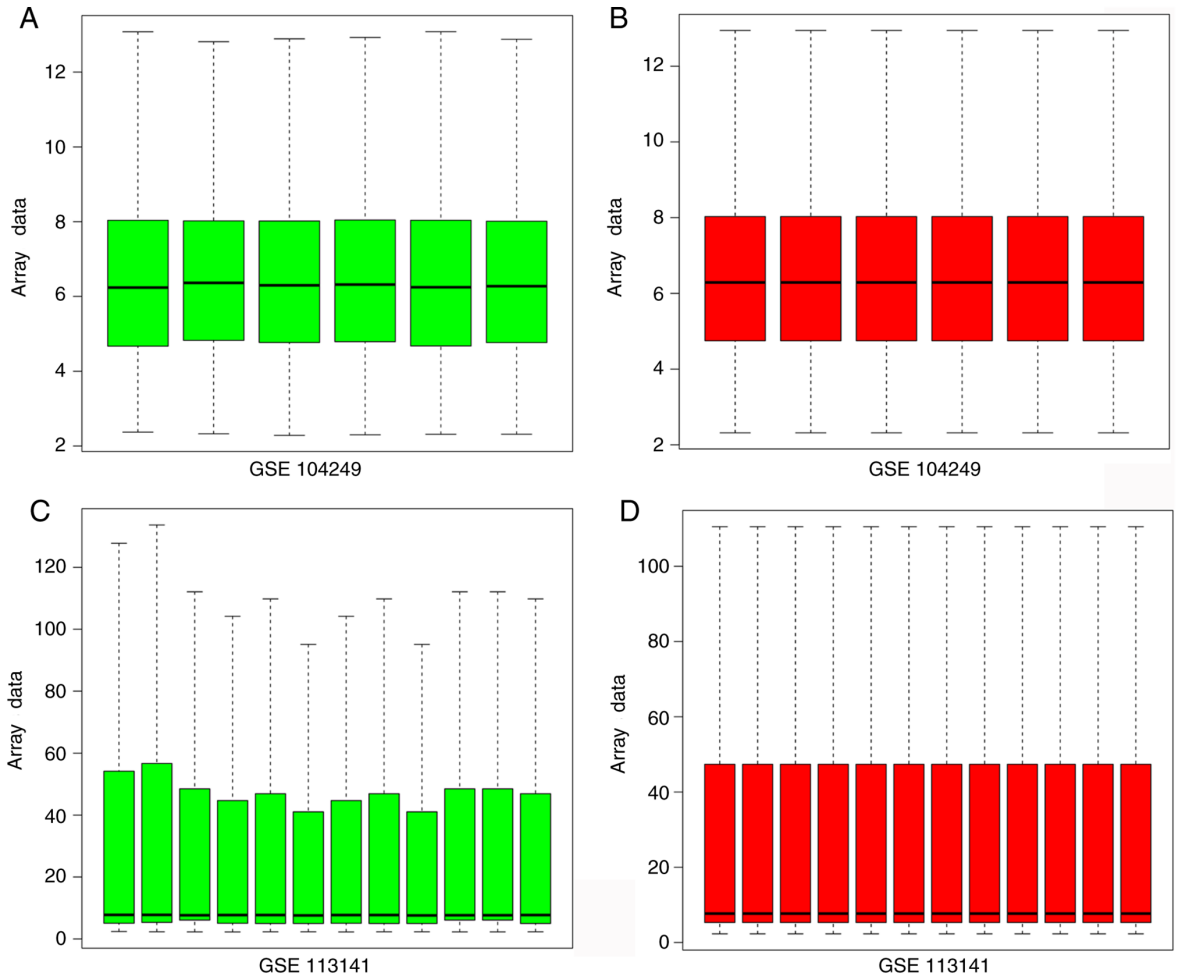

Figure 1. Homogenization of the raw data of GSE113141 and GSE104249. (A) Raw data of GSE104249 and (B) homogenization treatment. (C) Raw data of GSE113141 and (D) homogenization treatment.

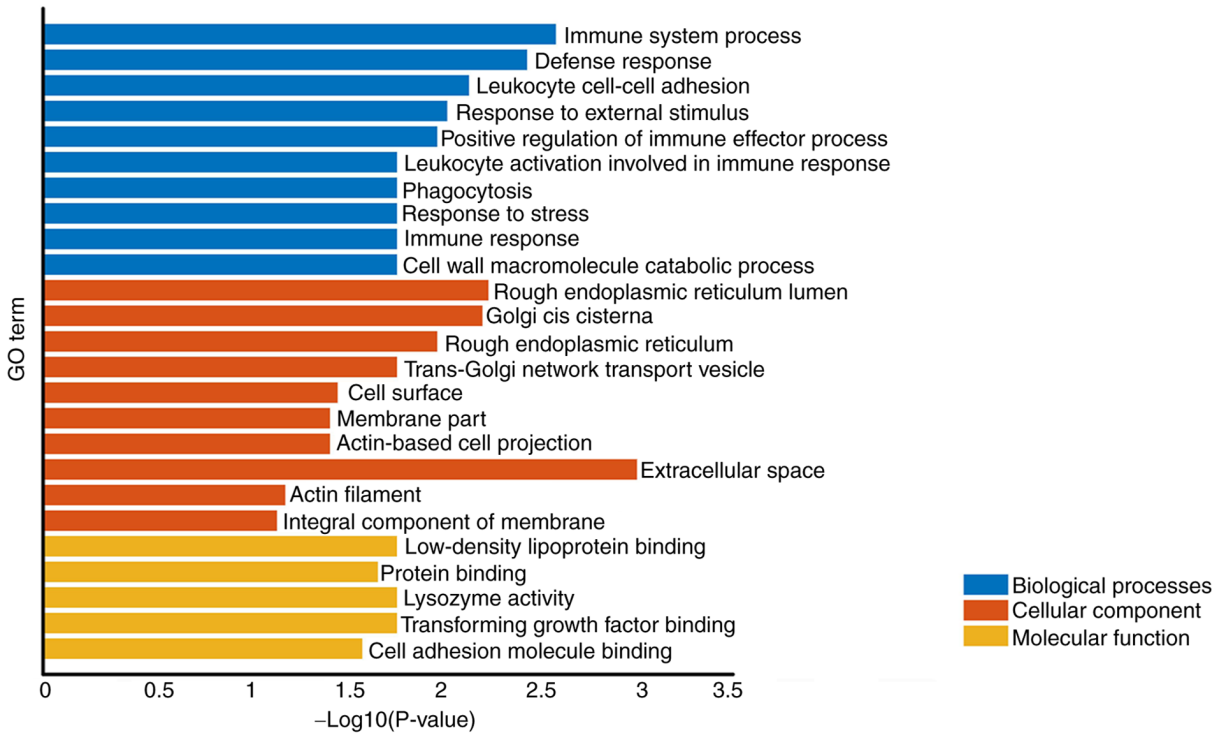

Figure 2. GO analysis. GO, Gene Ontology.

Table I. Enrichment analysis.

A, Biological processes

Term	Description	Gene count	P-value
Immune system process	GO:0002376	10	0.00250
Defense response	GO:0006952	8	0.00350
Leukocyte cell-cell adhesion	GO:0007159	3	0.00690
Response to external stimulus	GO:0009605	9	0.00890
Positive regulation of immune effector process	GO:0002699	4	0.01000
Leukocyte activation involved in immune response	GO:0002366	3	0.01600
Phagocytosis	GO:0006909	3	0.01600
Response to stress	GO:0006950	10	0.01600
Immune response	GO:0006955	6	0.01600
Cell wall macromolecule catabolic process	GO:0016998	2	0.01600

B, Cellular component

Term	Description	Gene count	P-value
Extracellular space	GO:0005615	7	0.00097
Rough endoplasmic reticulum lumen	GO:0048237	2	0.00550
Golgi *cis* cisterna	GO:0000137	2	0.00590
Rough endoplasmic reticulum	GO:0005791	3	0.01000
Trans-Golgi network transport vesicle	GO:0030140	2	0.01600
Cell surface	GO:0009986	5	0.03200
Membrane part	GO:0044425	13	0.03500
Actin-based cell projection	GO:0098858	3	0.03500
Actin filament	GO:0005884	2	0.05900
Integral component of membrane	GO:0016021	10	0.06500

C, Molecular function

Term	Description	Gene count	P-value
Lysozyme activity	GO:0003796	2	0.01600
Low-density lipoprotein particle binding	GO:0030169	2	0.01600
Transforming growth factor β binding	GO:0050431	2	0.01600
Protein binding	GO:0005515	14	0.02000
Cell adhesion molecule binding	GO:0050839	3	0.02400

GO, Gene Ontology.

GSE138382; this was also predicted to target *TYROBP*. These results demonstrated miR-628-5p/*TYROBP* may be used as an AD biomarker and molecular drug candidate.

High expression levels of TYROBP in APP/PS1 mice. RT-qPCR verification was performed using samples taken from mice (three APP/PS1 and three normal) and patients with AD. Analysis using RT-qPCR indicated that *TYROBP* was increased in APP/PS1 mice (Fig. 6A). Low miR-628-5p expression levels were detected in blood from patients with AD (Fig. 6A and B), which was consistent with GSE147232 (a miRNA microarray profile in the plasma of patients with mild cognitive impairment due to AD). Western blot analysis also confirmed that TYROBP, APP and Aβ were more highly expressed in APP/PS1 mice compared with normal mice (Fig. 6C and D). These results demonstrated that high expression of TYROBP fulfilled important roles in AD.

Increased miR-628-5p expression levels inhibit TYROBP in vitro. The transfection efficiency of miR-628-5p was confirmed by RT-qPCR. U251 cells transfected with miR-628-5p mimic demonstrated increased expression levels of miR-628-5p (Fig. 6E), whereas those transfected with miR-628-5p inhibitor exhibited upregulated *TYROBP*,

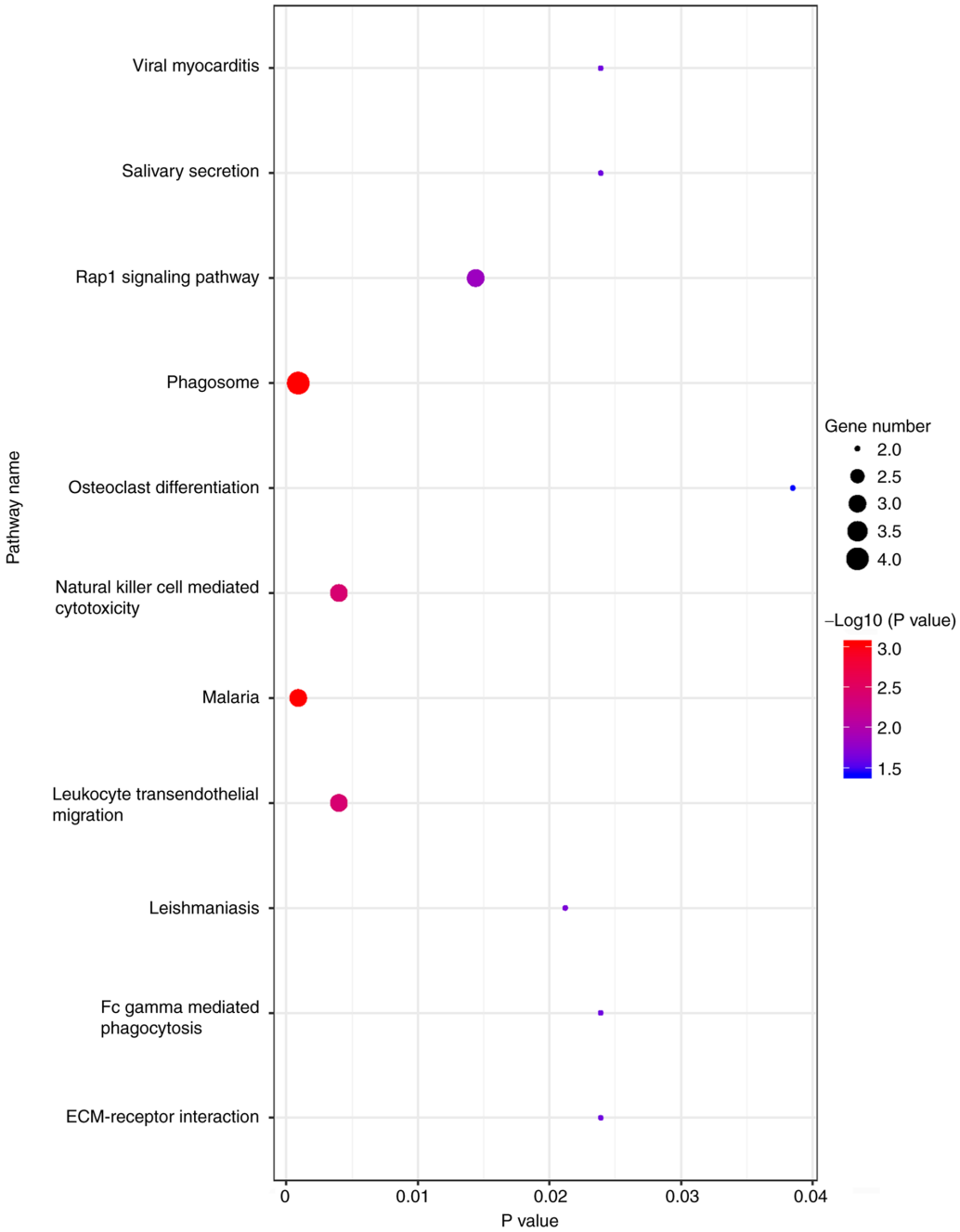

Figure 3. Kyoto Encyclopedia of Genes and Genomes analysis.

compared with the control. Western blot analysis demonstrated that decreased expression of miR-628-5p resulted in the upregulation of TYROBP, APP and Aβ compared with control group (Fig. 6F). These results demonstrated that high expression of miR-628-5p could inhibit TYROBP in U251 cells.

TYROBP targeting by miR-628-5p. Dual-luciferase reporter analysis demonstrated that co-transfection with miR-628-5p mimics significantly decreased the luciferase activity of the wild-type TYROBP reporter compared with that in the normal or mimic inhibitor samples and the mutant reporter (Fig. 7). These results demonstrated that miR-628-5p had binding sites with TYROBP and could inhibit translation of TYROBP in AD.

Discussion

AD has become one of the worldwide disorders involving central nervous system neurodegeneration and cognitive decline (27). However, its detailed molecular pathogenesis remains unclear. Although a number of hypotheses such as the cholinergic hypothesis (28), amyloid hypothesis (29) and tau hypothesis (30) have been proposed, the amyloid hypothesis is the most widely accepted (29). A number of drugs, including Semagacestat (4) and Tramiprosate (5) have been developed to inhibit Aβ; however, results have been unsatisfactory. For example, Semagacestat failed phase III clinical trials for AD treatment (4). Thus, further studies on the molecular pathogenesis of AD and novel drug targets are necessary.

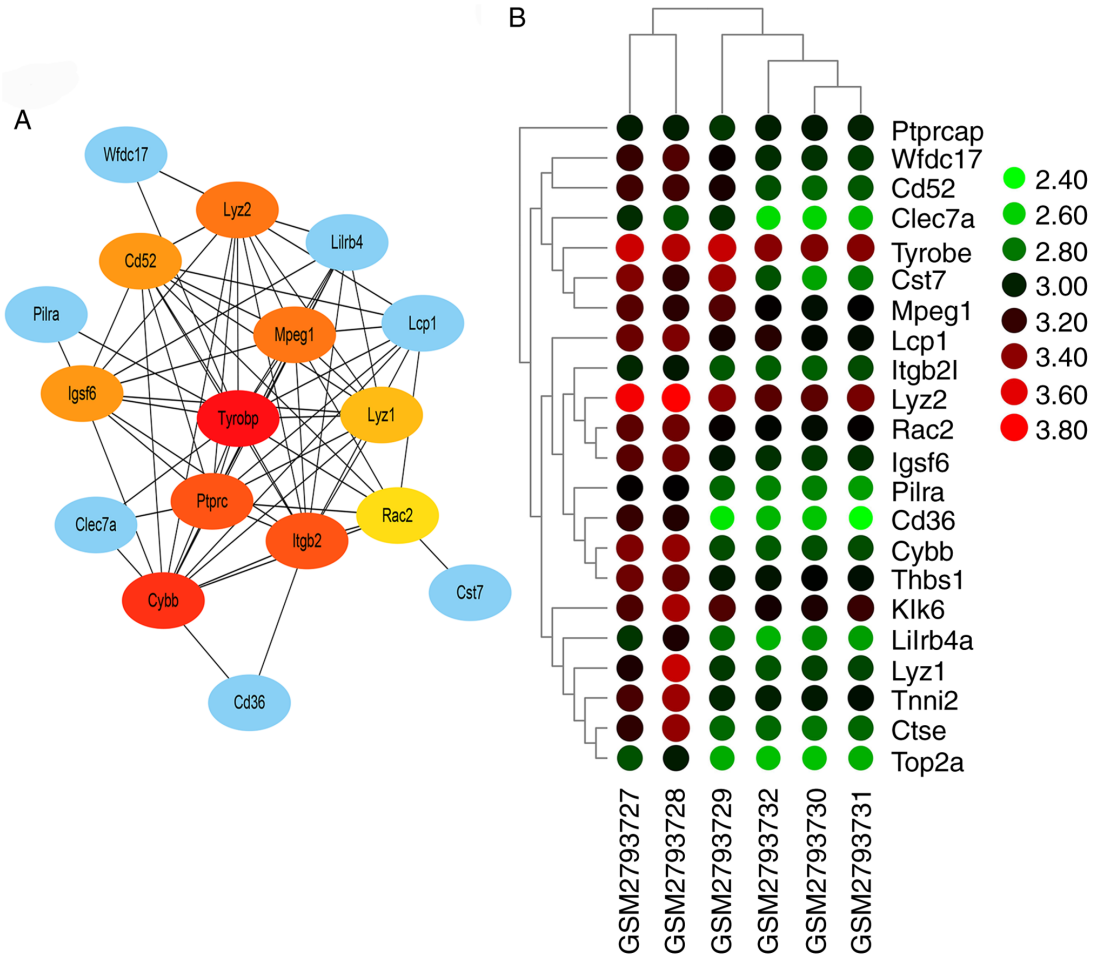

Figure 4. PPI network and heatmap of hub genes. (A) PPI network of all hub genes. (B) Heatmap of hub genes. Color gradient indicates degree score. Green, increased gene expression; red, decreased gene expression. PPI, protein-protein interaction.

Second-generation sequencing technology provides a fast method to screen DEGs between normal and impaired tissue such as brain, liver and kidney (14). Differential expression levels of both coding and non-coding RNAs may provide novel biomarkers for diagnosis and treatment targets (31). However, the abundance of DEGs obtained by this technique may mask core pathogenic genes. In addition, 'junk' information caused by individual differences (17) may be included among sequencing results. Therefore, normalization of raw data and integration analysis are necessary to provide reliable data for bioinformatics analysis.

The present GO analysis indicated that biological processes of AD were associated with immune and inflammatory responses. Neuro-inflammation has been reported to be involved in the progress of AD (32). Microglia in the brain produce pro-inflammatory cytokines to activate the inflammatory response. Moreover, NLR pyrin family domain containing 3 (NLRP3) has been reported to be activated by Aβ (33); activated NLRP3 can enhance AD progression via the chronic inflammatory response. In addition, the complement system is a family of key proteins that regulate the immune response and is considered to be the first line of homeostasis maintenance (34). Members of the complement system have also been found to have high expression levels in patients with AD. For example, C1q protein expression levels, associated with the classical complement pathway, are upregulated following activation by Aβ, and cause neuronal atrophy (35). Another study indicated that inhibiting C1q decrease synapse loss in mice (36).

Following bioinformatics analysis, *TYROBP* was predicted as a hub gene for AD. High expression levels of *TYROBP* in AD have previously been reported (37), which is consistent with previous results from second generation sequencing (15). However, previous research has focused on Aβ42, τ and TREM2 instead of TYROBP (38). Consistent with the present GO analysis, TYROBP serves as a core molecule in the immune system, particularly as the adapter for TREM2 and CRs, which control signal transduction (39). TREM2 and CR3 have been demonstrated to regulate the pathogenesis of AD (39). In addition, TYROBP inhibits inflammatory responses via down-regulation of microglia-mediated cytokine production (40). Based on the amyloid hypothesis, a number of drugs have been developed to inhibit Aβ. TYROBP may downregulate Aβ and clear apoptotic neurons by enhancing microglial phagocytic activity (41). To the best of our knowledge, the present study is the first to use bioinformatics analysis to predict *TYROBP* as a hub gene in AD. *TYROBP* may be a novel AD diagnosis biomarker and treatment target.

Previous studies have reported the function of TYROBP in AD (42,43). Although the detailed mechanism underlying

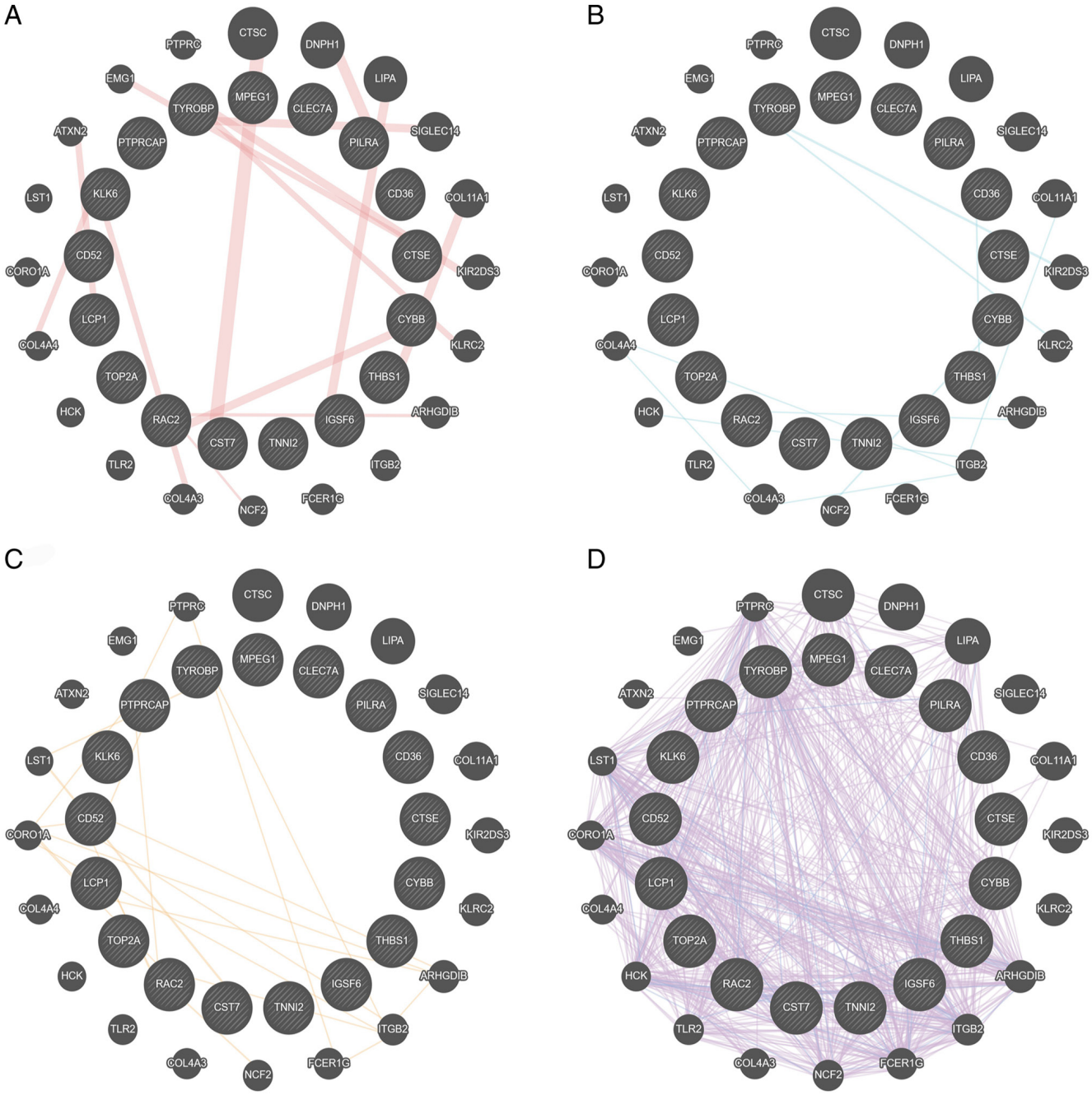

Figure 5. GeneMANIA analysis of co-expressed genes. (A) Physical interaction, (B) pathway, (C) prediction and (D) co-expression analysis of differentially expressed genes.

the cognitive decline of AD remains unknown, a partial loss of the colony stimulating factor 1 receptor (CSF1R)/TYROBP signaling pathway has been reported in neurological phenotypes (44). The immune response is reported to serve an important role during AD progression (45). TYROBP may mediate immune cell phagocytosis by regulating CSF1R and by interfering with macrophage proliferation, leading to white matter disease, which is clinically characterized by behavioral, cognitive and motor abnormalities (46). In addition, Haure-Mirande *et al* (41) suggested that TYROBP slows, arrests or prevents the development of sporadic late-onset AD (LOAD). The complement system is activated in AD (41). Deletion of TYROBP in a tauopathy mouse model downregulates C1q expression levels, leading to elevated learning behavior (retention tests) and synaptic function (47). Therefore, decreased expression levels of complement by TYROBP may be beneficial during AD pathology by improving learning behavior and synaptic function. Sekiya *et al* (38) found that glial expression of TYROBP promotes τ-mediated neurodegeneration and affects LOAD; furthermore, *TYROBP* was identified as a potential target gene by comparing human AD profiles, which is similar to the results of the present study.

miRNAs are a class of non-coding RNA molecule that inhibit translation or cause degradation of target mRNAs (48). To date, miR-628-5p has not been reported to participate in

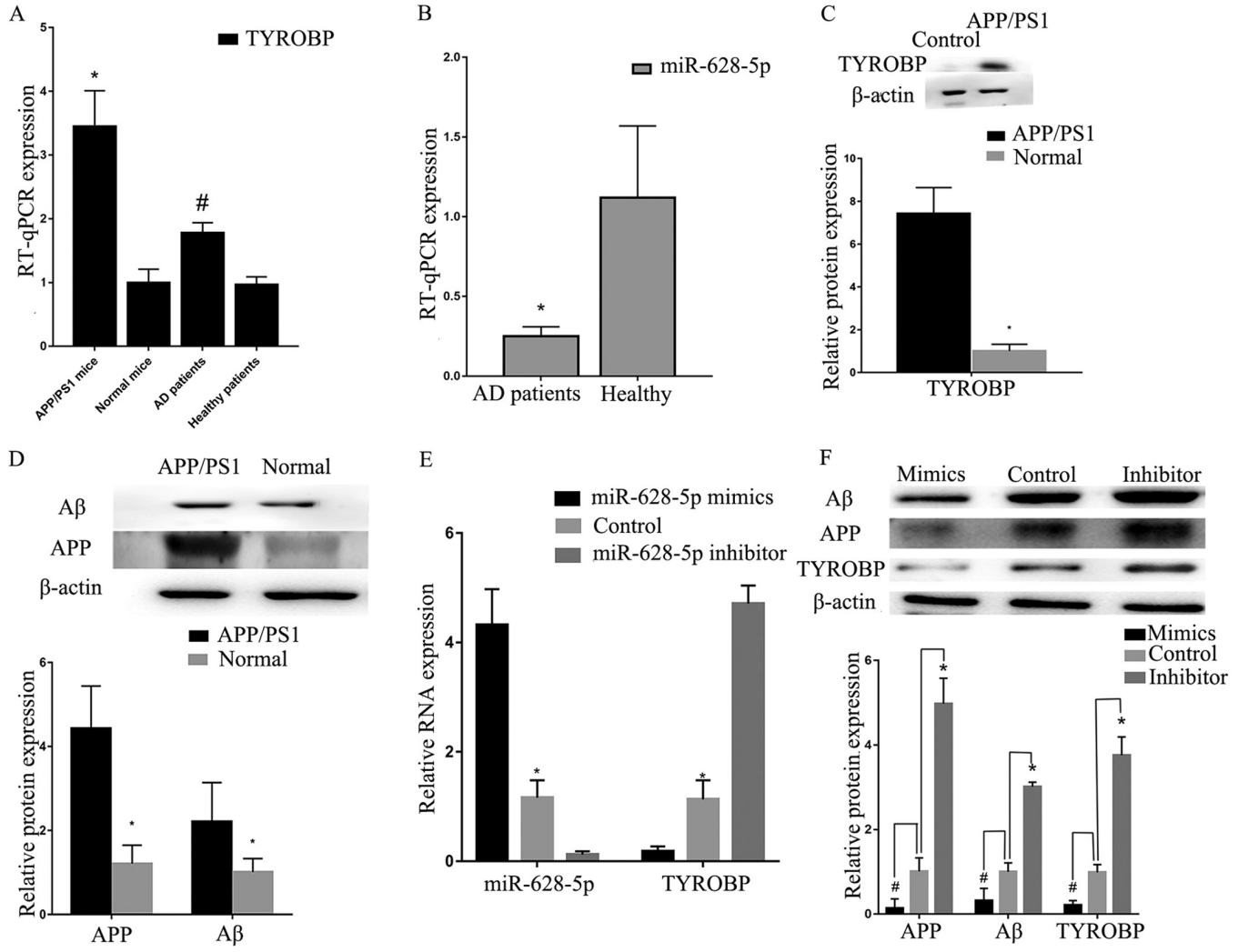

Figure 6. Validation of the hub gene *TYROBP* and miR-628-5p. (A) RT-qPCR confirmed that *TYROBP* is highly expressed in APP/PS1 transgenic mice (n=3) and patients with AD (n=10). (B) RT-qPCR confirmed low miR-628-5p expression levels in patients with AD. High expression levels of (C) TYROBP and (D) APP and Aβ in APP/PS1 transgenic mice was confirmed via western blot analysis. (E) RT-qPCR confirmed miR-628-5p transfection efficiency in U251 cells. (F) High expression levels of TYROBP, APP and Aβ were assessed by western blot analysis in U251 cells transfected with miR-628-5p inhibitor. *P<0.05 and #P<0.05 vs. respective control. TYROBP, transmembrane immune signaling adaptor TYROBP; miR, microRNA; RT-q, reverse transcription-quantitative; AD, Alzheimer's disease; APP, amyloid β precursor protein; Aβ, amyloid β.

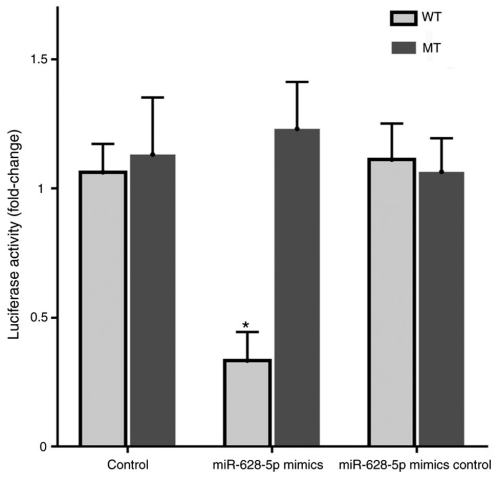

Figure 7. Association between miR-628-5p and TYROBP levels in 293T cells. Luciferase expression levels of WT TYROBP 3' untranslated region in miR-628-5p mimics was lower compared with that in the other groups. *P<0.05 vs. control. miR, microRNA; TYROBP, transmembrane immune signaling adaptor TYROBP; WT, wild-type; MT, mutant.

AD. Previously, miR-628-5p has been reported to inhibit glioblastoma cell proliferation and migration by targeting high mobility group box 3 (49); it can also decrease the proliferation of prostate (50) and epithelial ovarian cancer cells (51) by targeting fibroblast growth factor receptor 2 and inhibiting glioma proliferation by binding DEAD-box helicase 59 (52). Therefore, miR-628-5p may serve as a suppressor miRNA targets TYROBP, highlighting the potential of TYROBP as a novel therapeutic target for AD.

To the best of our knowledge, the present study is the first to use bioinformatics analysis and experimental confirmation to predict that miR-628-5p may inhibit the expression of AD-associated proteins. miR-628-5p/*TYROBP* may serve as a novel molecular diagnostic marker and candidate therapeutic target for AD.

Acknowledgements

Not applicable.

Funding

No funding was received.

Availability of data and materials

The datasets used and/or analyzed during the current study are available from the corresponding author on reasonable request.

Authors' contributions

ML and LY conceived and designed the study. SL, CM, XW and YS performed the experiments and collected the data. ML, HL and ZG analyzed and interpreted the data. ML performed experiments and drafted the manuscript. All authors read and approved the final manuscript.

Ethics approval and consent to participate

All experiments involving animals were approved by The Changchun University of Chinese Medicine Animal Care and Use Committee. RNA extraction, RNA reverse transcription and RT-qPCR validation involving patients' blood was approved by the Ethics Committee of Changchun University of Chinese Medicine.

Patient consent for publication

Not applicable.

Competing interests

The authors declare that they have no competing interests.

References

1. Weiner MW, Veitch DP, Aisen PS, Beckett LA, Cairns NJ, Green RC, Harvey D, Jack CR, Jagust W, Liu E, *et al*: The Alzheimer's disease neuroimaging initiative: A review of papers published since its inception. Alzheimers Dement 9: e111-e194, 2013.
2. De Strooper B: Lessons from a failed γ-Secretase Alzheimer trial. Cell 159: 721-726, 2014.
3. Mudher A and Lovestone S: Alzheimer's disease-do tauists and baptists finally shake hands? Trends Neurosci 25: 22-26, 2002.
4. Karran E and De Strooper B: The amyloid cascade hypothesis: Are we poised for success or failure? J Neurochem 139 (Suppl 2): S237-S252, 2016.
5. Gervais F, Paquette J, Morissette C, Krzywkowski P, Yu M, Azzi M, Lacombe D, Kong X, Aman A, Laurin J, *et al*: Targeting soluble Abeta peptide with Tramiprosate for the treatment of brain amyloidosis. Neurobiol Aging 28: 537-547, 2007.
6. Aisen PS, Gauthier S, Ferris SH, Saumier D, Haine D, Garceau D, Duong A, Suhy J, Oh J, Lau WC and Sampalis J: Tramiprosate in mild-to-moderate Alzheimer's disease - a randomized, double-blind, placebo-controlled, multi-centre study (the Alphase Study). Arch Med Sci 7: 102-111, 2011.
7. Tomasello E, Olcese L, Vely F, Geourgeon C, Bléry M, Moqrich A, Gautheret D, Djabali M, Mattei MG and Vivier E: Gene structure, expression pattern, and biological activity of mouse killer cell activating receptor-associated protein (KARAP)/DAP-12. J Biol Chem 273: 34115-34119, 1998.
8. Hamerman JA, Ni M, Killebrew JR, Chu CL and Lowell CA: The expanding roles of ITAM adapters FcRgamma and DAP12 in myeloid cells. Immunol Rev 232: 42-58, 2009.
9. Lanier LL, Corliss BC, Wu J, Leong C and Phillips JH: Immunoreceptor DAP12 bearing a tyrosine-based activation motif is involved in activating NK cells. Nature 391: 703-707, 1998.
10. Paloneva J, Kestila M, Wu J, Salminen A, Böhling T, Ruotsalainen V, Hakola P, Bakker AB, Phillips JH, Pekkarinen P, *et al*: Loss-of-function mutations in TYROBP (DAP12) result in a presenile dementia with bone cysts. Nat Genet 25: 357-361, 2000.
11. Varnum MM and Ikezu T: The classification of microglial activation phenotypes on neurodegeneration and regeneration in Alzheimer's disease brain. Arch Immunol Ther Exp (Warsz) 60: 251-266, 2012.
12. Sessa G, Podini P, Mariani M, Meroni A, Spreafico R, Sinigaglia F, Colonna M, Panina P and Meldolesi J: Distribution and signaling of TREM2/DAP12, the receptor system mutated in human polycystic lipomembraneous osteodysplasia with sclerosing leukoencephalopathy dementia. Eur J Neurosci 20: 2617-2628, 2004.
13. Satoh J, Shimamura Y and Tabunoki H: Gene expression profile of THP-1 monocytes following knockdown of DAP12, a causative gene for Nasu-Hakola disease. Cell Mol Neurobiol 32: 337-343, 2012.
14. Pareek CS, Smoczynski R and Tretyn A: Sequencing technologies and genome sequencing. J Appl Genet 52: 413-435, 2011.
15. Emilie F, Coelho JE, Zornbach K, Malik E, Baqi Y, Schneider M, Cellai L, Carvalho K, Sebda S, Figeac M, *et al*: Beneficial effect of a selective adenosine a_{2a} receptor antagonist in the APPswe/PS1dE9 mouse model of Alzheimer's Disease. Front Mol Neurosci 11: 235, 2018.
16. Wang W, Liu Q, Wang Y, Piao H, Li B, Zhu Z, Li D, Wang T, Xu R and Liu K: Integration of gene expression profile data of human epicardial adipose tissue from coronary artery disease to verification of hub genes and pathways. Biomed Res Int 2019: 8567306, 2019.
17. You J, Qi S, Du Y, Wang C and Su G: Multiple bioinformatics analyses of integrated gene expression profiling data and verification of hub genes associated with diabetic retinopathy. Med Sci Monit 26: e923146, 2020.
18. Faivre E, Coelho JE, Zornbach K, Malik E, Baqi Y, Schneider M, Cellai L, Carvalho K, Sebda S, Figeac M, *et al*: Beneficial effect of a selective adenosine A_{2A} receptor antagonist in the APPswe/PS1dE9 mouse model of Alzheimer's disease. Front Mol Neurosci 11: 235, 2018.
19. Liu W, Sun F, Wan M, Jiang F, Bo X, Lin L, Tang H and Xu S: β-Sheet breaker peptide-HPYD for the treatment of Alzheimer's disease: Primary studies on behavioral test and transcriptional profiling. Front Pharmacol 8: 969, 2018.
20. Shim SR and Kim SJ: Intervention meta-analysis: Application and practice using R software. Epidemiol Health 41: e2019008, 2019.
21. Otto R, Schirrmeister W, Majeed RW, Greiner F, Lucas B, Röhrig R, Walcher F and Brammen D; AKTIN Research Group: Implementation of emergency department performance benchmarking using R and LaTeX. Stud Health Technol Inform 267: 238-246, 2019.
22. Huang DW, Sherman BT, Tan Q, Collins JR, Alvord WG, Roayaei J, Stephens R, Baseler MW, Lane HC and Lempicki RA: The DAVID gene functional classification tool: A novel biological module-centric algorithm to functionally analyze large gene lists. Genome Biol 8: R183, 2007.
23. Shannon P, Markiel A, Ozier O, Baliga NS, Wang JT, Ramage D, Amin N, Schwikowski B and Ideker T: Cytoscape: A software environment for integrated models of biomolecular interaction networks. Genome Res 13: 2498-2504, 2003.
24. Livak KJ and Schmittgen TD: Analysis of relative gene expression data using real-time quantitative PCR and the 2(-Delta Delta C(T)) method. Methods 25: 402-408, 2001.
25. McKhann G, Drachman D, Folstein M, Katzman R, Price D and Stadlan EM: Clinical diagnosis of Alzheimer's disease: Report of the NINCDS-ADRDA Work Group under the auspices of the department of health and human services task force on Alzheimer's disease. Neurology 34: 939-944, 1984.
26. Zimmermann M: Ethical guidelines for investigations of experimental pain in conscious animals. Pain 16: 109-110, 1983.
27. Shen J and Kelleher RJ III: The presenilin hypothesis of Alzheimer's disease: Evidence for a loss-of-function pathogenic mechanism. Proc Natl Acad Sci USA 104: 403-409, 2017.
28. Francis PT, Palmer AM, Snape M and Wilcock GK: The cholinergic hypothesis of Alzheimer's disease: A review of progress. J Neurol Neurosurg Psychiatry 66: 137-147, 1999.
29. Hardy J and Allsop D: Amyloid deposition as the central event in the aetiology of Alzheimer's disease. Trends Pharmacol Sci 12: 383-388, 1991.

30. Goedert M, Spillantini MG and Crowther RA: Tau proteins and neurofibrillary degeneration. Brain Pathol 1: 279-286, 1991.
31. Chen J, Qi Y, Liu CF, Lu JM, Shi J and Shi Y: MicroRNA expression data analysis to identify key miRNAs associated with Alzheimer's disease. J Gene Med 20: e3014, 2018.
32. Sagy-Bross C, Hadad N and Levy R: Cytosolic phospholipase A2α upregulation mediates apoptotic neuronal death induced by aggregated amyloid-β peptide1-42. Neurochem Int 63: 541-550, 2013.
33. Heneka MT, Kummer MP, Stutz A, Delekate A, Schwartz S, Vieira-Saecker A, Griep A, Axt D, Remus A, Tzeng TC, *et al*: NLRP3 is activated in Alzheimer's disease and contributes to pathology in APP/PS1 mice. Nature 493: 674-678, 2013.
34. Sarma JV and Ward PA: The compliment system. Cell Tissue Res 343: 227-235, 2011.
35. Rogers J, Cooper NR, Webster S, Schultz J, McGeer PL, Styren SD, Civin WH, Brachova L, Bradt B, Ward P, *et al*: Complement activation by beta-amyloid in Alzheimer disease. Proc Natl Acad Sci USA 89: 10016-10020, 1992.
36. Schöll M, Lockhart SN, Schonhaut DR, O'Neil JP, Janabi M, Ossenkoppele R, Baker SL, Vogel JW, Faria J, Schwimmer HD, *et al*: PET imaging of tau deposition in the aging human brain. Neuron 89: 971-982, 2016.
37. Jiang Y, Li Z, Ma H, Cao X, Liu F, Tian A, Sun X, Li X and Wang J: Upregulation of TREM2 ameliorates neuroinflammatory responses and improves cognitive deficits triggered by surgical trauma in Appswe/PS1dE9 mice. Cell Physiol Biochem 46: 1398-1411, 2018.
38. Sekiya M, Wang M, Fujisaki N, Sakakibara Y, Quan X, Ehrlich ME, De Jager PL, Bennett DA, Schadt EE, Gandy S, *et al*: Integrated biology approach reveals molecular and pathological interactions among Alzheimer's Aβ42, Tau, TREM2, and TYROBP in drosophila models. Genome Med 10: 26, 2018.
39. Haure-Mirande JV, Audrain M, Fanutza T, Kim SH, Klein WL, Glabe C, Readhead B, Dudley JT, Blitzer RD, Wang M, *et al*: Deficiency of TYROBP, an adapter protein for TREM2 and CR3 receptors, is neuroprotective in a mouse model of early Alzheimer's pathology. Acta Neuropathol 134: 769-788, 2017.
40. Ma J, Jiang T, Tan L and Yu JT: TYROBP in Alzheimer's disease. Mol Neurobiol 51: 820-826, 2015.
41. Haure-Mirande JV, Wang M, Audrain M, Fanutza T, Kim SH, Heja S, Readhead B, Dudley JT, Blitzer RD, Schadt EE, *et al*: Integrative approach to sporadic Alzheimer's disease: Deficiency of Tyrobp in cerebral Abeta amyloidosis mouse normalizes clinical phenotype and complement subnetwork molecular pathology without reducing Abeta burden. Mol Psychiatry 24: 431-446, 2019.
42. Pottier C, Ravenscroft TA, Brown PH, Finch NA, Baker M, Parsons M, Asmann YW, Ren Y, Christopher E, Levitch D, *et al*: TYROBP genetic variants in early-onset Alzheimer's disease. Neurobiol Aging 48: 222.e9-222.e15, 2016.
43. Mori Y, Yoshino Y, Ochi S, Yamazaki K, Kawabe K, Abe M, Kitano T, Ozaki Y, Yoshida T, Numata S, *et al*: TREM2 mRNA expression in leukocytes is increased in Alzheimer's disease and schizophrenia. PLoS One 10: e0136835, 2015.
44. Kempthorne L, Yoon H, Madore C, Smith S, Wszolek ZK, Rademakers R, Kim J, Butovsky O and Dickson DW: Loss of homeostatic microglial phenotype in CSF1R-related Leukoencephalopathy. Acta Neuropathol Commun 8: 72, 2020.
45. Malik M, Parikh I, Vasquez JB, Smith C, Tai L, Bu G, LaDu MJ, Fardo DW, Rebeck GW and Estus S: Genetics ignite focus on microglial inflammation in Alzheimer's disease. Mol Neurodegener 10: 52, 2015.
46. Rademakers R, Baker M, Nicholson AM, Rutherford NJ, Finch N, Soto-Ortolaza A, Lash J, Wider C, Wojtas A, DeJesus-Hernandez M, *et al*: Mutations in the colony stimulating factor 1 receptor (CSF1R) gene cause hereditary diffuse leukoencephalopathy with spheroids. Nat Genet 44: 200-205, 2011.
47. Audrain M, Haure-Mirande JV, Wang M, Kim SH, Fanutza T, Chakrabarty P, Fraser P, St George-Hyslop PH, Golde TE, Blitzer RD, *et al*: Integrative approach to sporadic Alzheimer's disease: Deficiency of TYROBP in a tauopathy mouse model reduces C1q and normalizes clinical phenotype while increasing spread and state of phosphorylation of tau. Mol Psychiatry 24: 1383-1397, 2019.
48. Agarwal V, Bell GW, Nam JW and Bartel DP: Predicting effective microRNA target sites in mammalian mRNAs. Elife 4: e05005, 2015.
49. Chen WL, Jiang L, Wang JS and Liao CX: Circ-0001801 contributes to cell proliferation, migration, invasion and epithelial to mesenchymal transition (EMT) in glioblastoma by regulating miR-628-5p/HMGB3 axis. Eur Rev Med Pharmacol Sci 23: 10874-10885, 2019.
50. Srivastava A, Goldberger H, Dimtchev A, Marian C, Soldin O, Li X, Collins SP, Suy S and Kumar D: Circulatory miR-628-5p is downregulated in prostate cancer patients. Tumour Biol 35: 4867-4873, 2014.
51. Li M, Qian Z, Ma X, Lin X, You Y, Li Y, Chen T and Jiang H: miR-628-5p decreases the tumorigenicity of epithelial ovarian cancer cells by targeting at FGFR2. Biochem Biophys Res Commun 495: 2085-2091, 2018.
52. Xie P, Wang Y, Liao Y, Han Q, Qiu Z, Chen Y and Zuo X: MicroRNA-628-5p inhibits cell proliferation in glioma by targeting DDX59. J Cell Biochem 120: 17293-17302, 2019.